THE ABUNDANCES OF ULTRAHEAVY ELEMENTS IN THE COSMIC RADIATION

E. C. Stone[a], C. J. Waddington[b], W. R. Binns[c], T. L. Garrard[a], P. S. Gibner[a], M. H. Israel[c], M. P. Kertzman[b], J. Klarmann[c], and B. J. Newport[a,d]

a) California Institute of Technology; Pasadena, California 91125 USA
b) School of Physics and Astronomy, University of Minnesota; Minneapolis, Minnesota 55455 USA
c) Department of Physics and McDonnell Center for the Space Sciences, Washington University; St. Louis, Missouri 63130 USA
d) now at University of Chicago; Chicago, Illinois 60637 USA

Abstract

Analysis of a new, higher resolution data set from the Heavy Nuclei Experiment on the HEAO-3 spacecraft has yielded the cosmic ray abundances relative to iron of odd-even element pairs with atomic number, Z, in the range $33 \leq Z \leq 60$. The abundances are consistent with a solar-system source provided an allowance is made for a source fractionation based on first ionization potential (FIP). However, extending this analysis to element groups with $Z > 60$, we find enhancements of the Pt group ($74 \leq Z \leq 80$) abundance relative to the solar system and a corresponding increase in the largely secondary nuclei in the range $62 \leq Z \leq 73$, in agreement with recent Ariel-6 results. These abundances suggest an enhancement of the r-process contribution to the source of the $Z > 60$ nuclei.

1. Introduction. We have recently identified a subset of our data with improved resolution and statistics in the region of the charge spectrum from 40 to 60 [1] where good resolution has not previously been achieved. We will discuss this new result in the context of two charge regions, 34 to 60 (Fig. 1), where we have even element resolution; and above 60 (Fig. 2), where the even elements are not well resolved. The data below charge 40 are presented primarily to demonstrate agreement with the previously published data [2-4].

This data set consists only of nuclei which have energy greater than about 1 GeV/amu. All events are required to have consistency between two ion chambers on opposite sides of a Cherenkov detector, and between the ion chambers and the Cherenkov [5]. Charge is determined for these events from the Cherenkov signal alone, with the ionization signal used only for consistency checks. The number of iron nuclei corresponding to this data set is 8.0×10^6.

2. Observations: $34 \leq Z \leq 60$. Figure 1 shows the charge histogram of this data set for Z=30 through 42 (upper) and for 40 through 62 (lower). Superimposed are smooth curves which show the results of fitting these histogram data with a gaussian resolution function as described by Newport [1]. The systematic error in the quoted abundances due to the choice of fitting functions and parameters is roughly 12% rms. The systematic errors are correlated, however, since a fit which yields an increased abundance for one element must yield a reduced abundance for neighboring elements in order to conserve particles. This uncertainty is in addition to the tabulated statistical errors. The preliminary abundances derived from this fitting procedure are plotted in Fig. 3a in charge pairs, the abundance of each even charge being combined with the odd charge immediately below it, with the exceptions of those for Z=39 to 41 which are combined and plotted as a single point and that for 42 which is plotted by itself. The abundances are presented in this fashion since there may still be a residual tail extending down from the more abundant even charges which is not deconvolved using the gaussian fitting function.

3. Observations: $Z > 60$. In the $Z > 60$ charge region (see Fig. 2), we do not see the well resolved peaks observed below 60. A likely cause for the lack of peaks is a larger

fraction of odd Z nuclei. Other possible causes include a greater fraction of low energy nuclei, resolution worsened by instrumental problems such as mapping, and deviations from Z^2 scaling in the Cherenkov response. These problems are compounded by poor statistics. As a result, we have grouped the nuclei into four charge regions rather than fitting individual elements. The relative abundances of these groups are shown in Fig. 3. The groups are labeled "LS", $61.5 \leq Z \leq 69.5$; "HS", 69.5 to 73.5; "Pt", 73.5 to 80.5; and "Pb", 80.5 to 86.5.

<u>4. Comparisons.</u> In Fig. 3a (and in Table 1), we compare our new results with our previously published abundances [2-4] and find generally good agreement with these earlier data sets. In the Bangalore $Z \leq 42$ data [2], we required better knowledge of the particle energy, and could correct the Cherenkov signal to its high energy value. In that data set we had better resolution but significantly less statistical precision. For the earlier $50 \leq Z \leq 58$ data set [3], we required an energy above about 2.5 GeV/nuc, but events with only one ion chamber were accepted. These data are comparable in both resolution and statistics to those presented here. In Binns *et al.*, '85 [4], the energy cut was ~1.5 GeV/nuc (cutoff rigidity ≥ 5 GV) and only one ion chamber was required because of the extreme rarity of the $Z > 60$ events. That data set had statistical weight comparable to this one. Binns [6] has reviewed data from [1-4] in greater detail.

After a small correction for interactions in the lids of the detector system as described by Newport [1], we also find good agreement (Fig. 3b, Table 1) with the Ariel-6 abundances [7]. To compare these abundances with those of a solar system source, we have taken the Anders and Ebihara meteoritic abundances [8], fractionated according to the Letaw *et al.* step-FIP model [9], and propagated to earth using a leaky box model [1,10] with a rigidity dependent path length. The ratio

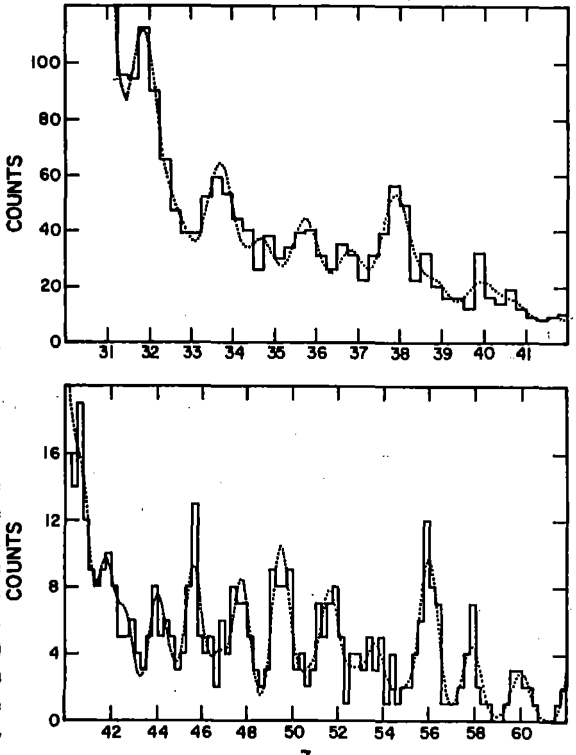

Figure 1. Charge histograms. The dotted lines show the fit from which the abundances are determined

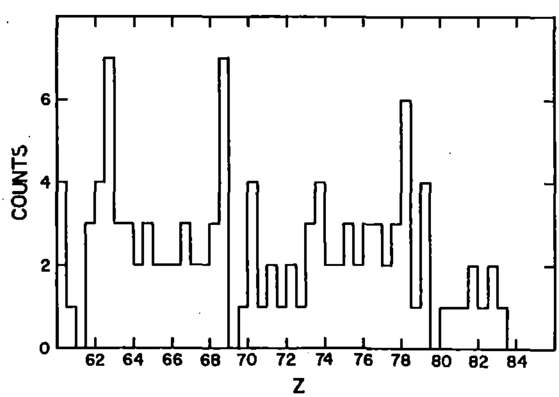

Figure 2. Charge histogram for $Z > 60$

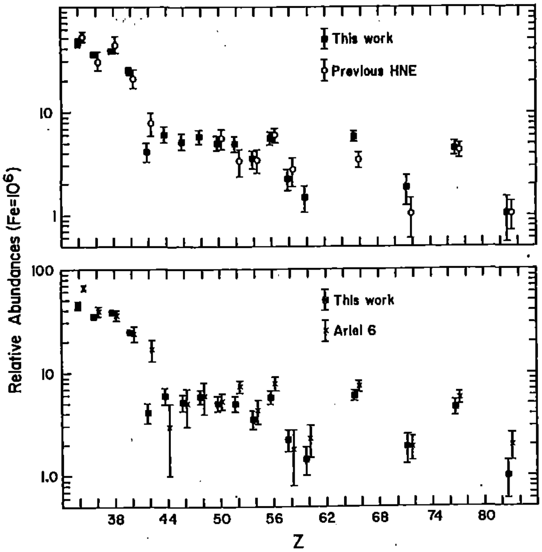

Figure 3. A comparison of relative abundances with previous HNE publications and Ariel 6 work. Plotted as a function of atomic number Z

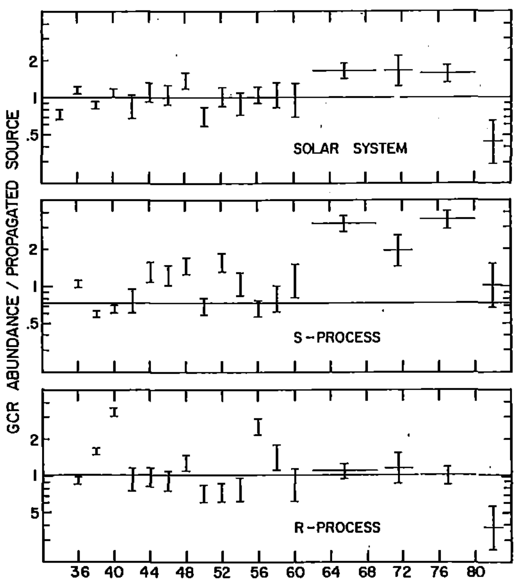

Figure 4. Ratios of measured abundances to calculated abundances using 3 different models for the source

of our measured abundances to these fractionated and propagated solar system abundances is plotted versus charge in the upper panel of Fig. 4. There is agreement to within ±30% from charge 34 to 60. In particular, this is true for the newly measured abundances in the 40's. Similar comparisons to pure r- and pure s-process sources [4] are shown in the lower panels of Fig. 4. The observations in this charge range are inconsistent with a source composition which is dominated by either r-process or s-process material. The best fit is obtained with a source enriched slightly in r-process material, i.e., a source having an r- to s-process ratio of $1.22^{+0.25}_{-0.21}$, relative to the solar system. Note that the observations do not exclude a source containing the same mixture of r- and s-process material as in the solar system. Comparisons using no FIP or using an exponential-FIP fractionation give poorer agreement for any of the three source possibilities.

In the Z>60 region, the agreement with the solar system is not as good. If we assume a solar system source, the observed Pb abundance is notably lower while the Pt, HS, and LS abundances are higher than predicted. One possible explanation for the low Pb abundance is the suggestion of Grevesse and Meyer [11] that the photospheric abundance of Pb is about 0.63 of the standard meteoritic [8] abundance. Another is a volatility related fractionation [4].

The high abundance of the Pt group appears to indicate an additional admixture of r-process source material in this charge region. The high HS, LS abundances lend additional credence to the idea of an enhancement in the r-process component. This conclusion does not depend on the step-FIP model used; the enhancement also is seen if the FIP correction is omitted.

If we assume an r-process source, then the "secondary" (LS, HS) to "primary" (Pt) ratio is consistent with the standard leaky box model. No more elaborate models are justified, especially in view of the paucity of the statistics and the uncertainties in the cross-sections (see OG7.2-11, 12; this conference). We note that our previously published HEAO data [4] have smaller LS and HS abundances. The difference may indicate an energy dependence in these abundance ratios. Such an energy dependence might also explain the lack of resolution in the 60's for this data set.

We also note that this data set does not contain an actinide. The one actinide in Binns *et al.*, '82 [12], using a data set of greater statistical significance (corresponding to $\sim 18 \times 10^6$ Fe events), did not meet the geometry criteria required for this work. Neither result is inconsistent with the Ariel work [7].

5. Conclusions. We find that the cosmic ray abundances in the Z=34 to 60 region (including the new 40 to 60 data) are in generally good agreement with solar system abundances with a step-FIP fractionation model applied, as we had earlier concluded looking separately at the 30's and 50's. We have seen that the cosmic ray source is definitely not dominated by the r-process for $Z \leq 60$. The newly resolved elements in the charge region 40 to 48 are largely secondary assuming a solar system source and the observations agree well with the calculations; in this charge region it is unnecessary to invoke anything more elaborate than the standard leaky box model.

In the $Z > 60$ region, abundances of the Pt group and the corresponding "secondary" groups (LS, HS) seem to indicate an enhancement of r-process nuclei compared to the solar system.

4. Acknowledgements. This research was supported in part by NASA under grants NAG 8-498, 500, and 502 and NGR 05-002-160, 24-005,050, and 26-008-001.

Table 1
Relative Abundances ($Fe=10^6$)

element	this work	Ariel [7]	previous [2,3,4]
33-34	44.9±4.1	66 ±5	52 ±6
35-36	35.1±2.4	39 ±4	30 ±8
37-38	38.1±2.4	36 ±4	43 ±6
39-40-41	24.7±1.9	32 ±4	21 ±5
42	4.2±0.9	9 ±4	8 ±2
43-44	6.1±1.1	3 ±2	- -
45-46	5.2±0.9	5 ±2	- -
47-48	5.9±0.9	6 ±1.3	- -
49-50	5.1±0.8	3 ±1.0	5.7 ±1.3
51-52	5.1±0.9	7.4±1.0	3.0 ±1.0
53-54	3.6±0.7	4.3±1.1	3.5 ±0.9
55-56	5.8±0.9	7.9±1.2	6.2 ±1.0
57-58	2.3±0.5	1.8±1.0	2.8 ±0.9
59-60	1.5±0.4	2.3±0.8	- -
LS	6.0±0.7	7.4±0.9	3.54±0.63
HS	$1.9^{+0.6}_{-0.5}$	1.9±0.5	$1.04^{+0.45}_{-0.33}$
Pt	4.6±0.8	5.7±0.8	4.38±0.71
Pb	$1.0^{+0.5}_{-0.4}$	2.0±0.6	$1.04^{+0.45}_{-0.33}$

References

1. Newport B. J., Thesis, California Institute of Technology, 1986.
2. Binns *et al.*, *Proc. 18th ICRC (Bangalore)*, **9**, 1983, 106.
3. Stone *et al.*, *Proc. 18th ICRC (Bangalore)*, **9**, 1983, 115.
4. Binns W. R., N. R. Brewster, D. J. Fixsen, T. L. Garrard, M. H. Israel, J, Klarmann, B. J. Newport, E. C. Stone, and C. J. Waddington, *Ap. J.*, **297**, 1985, 111.
5. Binns *et al.*, *Nucl. Instr. Meth.*, **185**, 1981, 415.
6. Binns W. R., "Ultra Heavy Nuclei in the Cosmic Radiation", **Genesis and Propagation of Cosmic Rays**, Reidel & Co., Dordrecht, 1987, in press
7. Fowler P. H., R. N. F. Walker, M. R. W. Masheder R. T. Moses, A. Worley, and A. M. Gay, to be pub. *Ap. J.*, March 1987.
8. Anders E. and M. Ebihara, *Geochim. et Cosmochim.*, **46**, 1982, 2363.
9. Letaw J. R., R. Silberberg, and C. H. Tsao, *Ap. J.*, **279**, 1984, 144.
10. Brewster *et al.*, *Ap. J.*, **294**, 1985, 419.
11. Grevesse N. and J. P. Meyer, *Proc. 19th ICRC (La Jolla)*, **3**, 1985, 5.
12. Binns *et al.*, *Ap. J.*, **261**, 1982, L117.